Validation of double diffusion schemes of microscopic fractional anisotropy

Henrik Lundell[1], Tim B. Dyrby[1], Penny L. Hubbard Cristinacce[2,3], Feng-Lei Zhou[2,4], Geoffrey J.M. Parker[2,3], and Sune N. Jespersen[5,6]

[1]Centre for Functional and Diagnostic Imaging and Research, Copenhagen University Hospital, Hvidovre, Denmark, [2]Centre for Imaging Sciences, The University of Manchester, United Kingdom, [3]Biomedical Imaging Institute, The University of Manchester, United Kingdom, [4]The School of Materials, The University of Manchester, United Kingdom, [5]CFIN/MINDLab, Aarhus University, Denmark, [6]Department of Physics and Astronomy, Aarhus University, Denmark

Target audience: Researchers with an interest in diffusion imaging, diffusion-MR method development, and tissue microstructural imaging.

Purpose: Diffusion sequences with two diffusion encoding blocks have recently been proposed to allow model free characterization of microscopic diffusion anisotropy, i.e. diffusion anisotropy of the individual water compartments insensitive to their directional dispersion[1-3]. For example, the d-PFG 5-design was shown to provide metrics of e.g. microscopic fractional anisotropy[4], μFA[5, 6], using 72 pairs of gradient directions. In contrast to FA, μFA in theory remains unaffected by the presence of fiber dispersion or crossing, and theoretically equals FA for single straight fiber bundles. The purpose of this work was to test the ability to distinguish μFA from macro FA in controllable phantoms, and then to evaluate the relative performance of different sampling schemes.

Theory: Double diffusion encoding (DDE) pulse sequences are constructed from ordinary diffusion sequences, but contain two diffusion weighting blocks separated by a mixing time. For long mixing times, it has been realized[1-3] that in macroscopically isotropic systems, the difference in diffusion signals between acquisitions with parallel and perpendicular wave vectors is proportional to the eccentricity of water compartments for long diffusion times, or proportional to the diffusion anisotropy of the water compartments for any diffusion time[4, 7, 8]. If there is an additional macroscopic anisotropy (i.e. a non-vanishing FA), it needs to be disentangled from the microscopic anisotropy, which can be done by combining parallel and perpendicular diffusion directions from an orientationally invariant isotropic sampling scheme, such as the d-PFG 5-design. In such a case, microscopic diffusion anisotropy ε can be found from the DDE signal $S(\mathbf{q}_1,\mathbf{q}_2)$ using Eq. (1), where χ denotes the set of

$$\varepsilon q^4 = \log\left(|\chi_{\parallel}|^{-1}\sum_{\chi_{\parallel}} S(q\hat{\mathbf{n}}_1, q\hat{\mathbf{n}}_2)\right) - \log\left(|\chi_{\perp}|^{-1}\sum_{\chi_{\perp}} S(q\hat{\mathbf{n}}_1, q\hat{\mathbf{n}}_2)\right) \quad (1)$$

$$\mu FA = \sqrt{3/2}\left(1 + MD^2\, 3\Delta^2/5\varepsilon\right)^{-1/2} \quad (2)$$

diffusion wave vectors $(\mathbf{q}_1,\mathbf{q}_2)$, and the sums are over $|\chi_{\parallel}|$ parallel and $|\chi_{\perp}|$ perpendicular combinations of gradient directions $(\hat{\mathbf{n}}_1,\hat{\mathbf{n}}_2)$. In addition to the d-PFG 5-design, we present here two additional designs found to fulfill Eq. (1). The first is the set of 15 pairs introduced in ref. [7], and the second is one hemisphere of the icosahedral vertices (ICO)). For the icosahedral set, the first sum in Eq. (1) is over parallel combinations, and the second sum is over combinations of distinct vertices, and the result is normalized by $1-\cos^2(63.44°)$ to account for the non-perpendicular angle (63.44°) between distinct vertex directions. Once ε has been estimated, μFA is found from Eq. (2), where MD is mean diffusivity[4].

Methods: A 4.7 T Agilent MRI scanner with a quadrature coil was used for data acquisition. Standard DTI as well as DDE images were collected from a phantom constructed from co-electrospun liquid filled hollow fibers with area weighted mean diameter of 13.4 μm as described in ref. [9]. The basic set up is seen in Fig. 1 and corresponds to a single planar fiber bundle in the z-axis of our reference system. DDE data were acquired with the three schemes described above, and repeated for two rotations of the schemes, yielding three data sets for each scheme: A (no rotation), B (90° rotation around the x-axis), and C (45° rotation around the y-axis). The raw diffusion data from some of these data sets were added to simulate crossing fibers, giving two additional data sets: AB (corresponding to two identical fiber bundles crossing at 90 degrees) and ABC (corresponding to three crossing identical fiber bundles). The DTI data were only acquired for one orientation of the gradient set, and the other 4 data sets were then constructed by rotating the diffusion tensor obtained from A. The DTI data set consisted of 24 directions acquired at b=1500 s/mm2 with a conventional PGSE (G = 0.49 T/m, Δ = 11 ms, δ = 3 ms), as well as five b=0 images. The DDE data sets used identical gradient strength and timing in two independent bipolar diffusion encodings on each side of the inversion pulse with a mixing time of 10 ms. Matrix size was 128x128x4, voxel size 0.25x0.25x3.0 mm, TR = 4 s and TE = 65 ms for both the PGSE and DDE acquisition. To facilitate a comparison, the number of averages was adjusted for each scheme to yield approximately the same number of images. Hence for the d-PFG 5-design, NEX=1, for DTI NEX=2, for ICO NEX=3 and for 15-dir NEX=5. In the following, data from a single ROI as shown in Fig. 1 is analyzed.

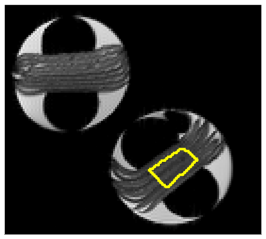

Fig. 1: Fiber phantoms and ROI definition (yellow square).

Results: Fig. 2 examines the dependence of μFA on fiber orientation/rotation among the schemes, as well as their comparison to the standard FA. It can be seen that all metrics are relatively robust against rotations, and they are approximately equal to the standard FA, as they should in the absence of orientational dispersion. Fig. 3 demonstrates the insensitivity of μFA to fiber dispersion, by plotting ROI averages for a single fiber (A), two crossing fibers (AB), and three crossing fibers (ABC). At the same time it is clear that FA is strongly reduced when more than one fiber bundle contributes.

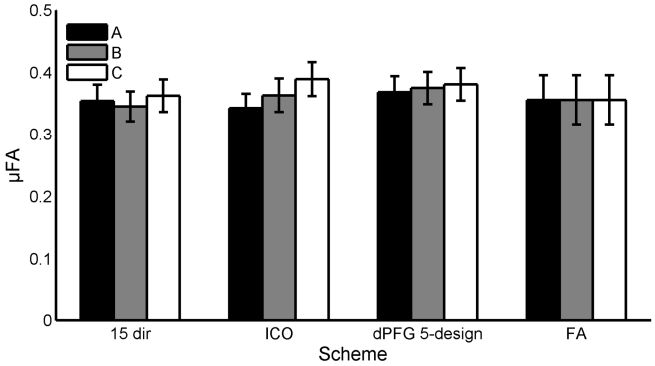

Fig. 2: Mean μFA over the ROI for each acquisition scheme and each fiber orientation. FA for A, B and C are identical by construction.

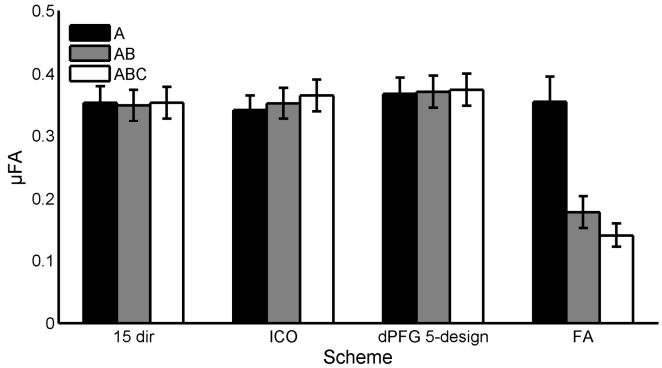

Fig. 3: Mean μFA over the ROI for each acquisition scheme and each fiber bundle configuration.

Discussion and conclusion: This study demonstrated that while FA is affected by compartment intrinsic properties as well as compartment dispersion, μFA disambiguates these two properties and equals FA with the effects of compartment dispersion removed. The difference between μFA and FA is a measure of dispersion. Thus DDE sequences can provide information complementary to that obtained from standard diffusion sequences, and should be helpful when interpreting diffusion data in terms of microstructure. The three proposed acquisition schemes perform similarly in terms of precision and accuracy, but further experiments are needed to evaluate more complex fiber configurations, the effect of extracellular compartments and real neuronal tissue. Funding: Lundbeck Foundation R83-A7548, Simon Fougner Hartmanns Familiefond and EU CONNECT.

References: 1. Cheng, Y., et al., J. Am. Chem. Soc., 1999. **121**(34). 2. Mitra, P.P., Phys. Rev. B, 1995. **51**(21). 3. Cory, D.G., et al., Polym. Prep. Am. Chem. Soc. Div. Polym. Chem., 1990. **31**. 4. Jespersen, S.N., et al., NMR Biomed, 2013. **26**(12). 5. Lasic, S., et al., Frontiers in Physics, 2014. **2**. 6. Jespersen, S.N., et al., Frontiers in Physics, 2014. **2**. 7. Lawrenz, M., et al., J. Magn. Reson., 2010. **202**(1). 8. Özarslan, E., et al., J. Chem. Phys., 2008. **128**(15). 9. Hubbard, P.L., et al., Magn. Reson. Med., 2014.